Geochemistry Geophysics Geosystems G3

AN ELECTRONIC JOURNAL OF THE EARTH SCIENCES

Published by AGU and the Geochemical Society

Data Brief

Volume 6, Number 1

14 January 2005

Q01001, doi:10.1029/2004GC000802

ISSN: 1525-2027

Sr-Nd isotope systematics in 14–28 Ma low-temperature altered mid-ocean ridge basalt from the Australian Antarctic Discordance, Ocean Drilling Program Leg 187

Sylwia Krolikowska-Ciaglo

Leibniz-Institut für Meereswissenschaften an der Universität Kiel, IFM-GEOMAR, Wischhofstrasse 1-3, 24148 Kiel, Germany

Now at Instytut Geologii, Uniwersytet im. Adama Mickiewicza, ul. Maków Polnych 16, 61-606 Poznań, Poland (skrolikowska@ifm-geomar.de)

Folkmar Hauff and Kaj Hoernle

Leibniz-Institut für Meereswissenschaften an der Universität Kiel, IFM-GEOMAR, Wischhofstrasse 1-3, 24148 Kiel, Germany (fhauff@ifm-geomar.de; khoernle@ifm-geomar.de)

[1] The effects of low-temperature alteration on the Rb-Sr and Sm-Nd isotope systems were investigated in 14–28 Ma mid-ocean ridge basalts recovered during Ocean Drilling Program (ODP) Leg 187 from the Australian Antarctic Discordance through comparison of pristine glass and associated variably altered basalts. Both Nd and Sm are immobile during low-temperature alteration, and $^{143}Nd/^{144}Nd$ displays mantle values even in heavily altered samples. In contrast, $^{87}Sr/^{86}Sr$ and Rb concentrations increase during seawater-rock interaction, which is especially apparent in single samples with macroscopically zoned alteration domains. The increase in $^{87}Sr/^{86}Sr$ roughly correlates with the visible degree of alteration, indicating a higher seawater/rock ratio in the more altered samples. Sr concentrations, however, do not systematically increase with increasing degree of alteration, most likely reflecting exchange of Sr in smectite interlayer sites. The degree of alteration in the uppermost oceanic crust of the Australian Antarctic Discordance is independent of crustal age. A comparison with literature data for young and old altered oceanic crust suggests that most low-temperature alteration occurs within a few million years after formation of the oceanic crust, probably reflecting greater fluid flux through the crust during its early history as a result of higher permeability and increased fluid circulation near the ridge.

Components: 8624 words, 7 figures, 4 tables.

Keywords: low-temperature alteration; basalts composition; oceanic crust; Rb-Sr and Sm-Nd isotope systems.

Index Terms: 1040 Geochemistry: Radiogenic isotope geochemistry; 1065 Geochemistry: Major and trace element geochemistry; 1039 Geochemistry: Alteration and weathering processes (3617).

Received 13 July 2004; **Revised** 28 September 2004; **Accepted** 11 November 2004; **Published** 14 January 2005.

Krolikowska-Ciaglo, S., F. Hauff, and K. Hoernle (2005), Sr-Nd isotope systematics in 14–28 Ma low-temperature altered mid-ocean ridge basalt from the Australian Antarctic Discordance, Ocean Drilling Program Leg 187, *Geochem. Geophys. Geosyst.*, *6*, Q01001, doi:10.1029/2004GC000802.

1. Introduction

[2] Ocean Drilling Program (ODP) Leg 187 [*Christie et al.*, 2001] mapped the paleoboundary between the Indian and Pacific mantle domains in a 14–28 Ma crustal profile immediately north of the Australian Antarctic Discordance (AAD), providing valuable constraints for the reconstruction and

evolution of this important mantle boundary [*Kempton et al.*, 2002]. The availability of variably altered basalt together with fresh basalt and fresh glass from a large number of drill sites that cover a substantial section of relatively young crust provide an excellent opportunity to investigate the temporal and the compositional effects of alteration in the uppermost oceanic crust through time.

[3] While high-temperature alteration of oceanic crust primarily takes place during and shortly after the formation of oceanic crust at spreading centers, low-temperature alteration (<50°C) may last over extended periods, affecting both the chemical composition of seawater and the crust. It is not known exactly how long the seawater-basalt interaction takes place. Numerous studies based on physical properties of basalts suggest that low-temperature alteration of the oceanic crust is progressive and age-dependent [e.g., *Johnson and Semyan*, 1994; *Zhou et al.*, 2001]. On the other hand, some mineralogical [*Talbi and Honnorez*, 2003] and isotopic [*Hauff et al.*, 2003] investigations imply that low-temperature alteration primarily occurs during the first few million years after crust formation and that only precipitation of carbonates has a major effect on the composition of the crust throughout its history on the seafloor [*Alt and Teagle*, 1999].

[4] Alteration studies of in situ ocean crust have thus far mainly focused on DSDP/ODP Sites 417/418 [*Staudigel et al.*, 1995; 1996], 735B [*Bach et al.*, 2001], 504B [*Alt et al.*, 1996a, 1996b; *Bach et al.*, 2003], Sites 801 and 1149 [*Kelley et al.*, 2003; *Hauff et al.*, 2003] and crustal xenoliths associated with intraplate volcanism [*Hoernle*, 1998; *Schmincke et al.*, 1998]. Previous studies of the alteration of oceanic crust have concentrated either on very young (<15 Ma) or old (>100 Ma) oceanic crust and crust of intermediate age (15–100 Ma) has been less extensive investigated. Here we report Rb, Sr, Sm, and Nd concentrations and Sr-Nd isotopic compositions of pristine glass, fresh and variably altered basalts from 11 Sites drilled into 14–28 Ma ocean crust during ODP Leg 187. The high fluid mobility of Sr and the relatively high Sr concentrations in seawater (8 ppm) in conjunction with large differences in $^{87}Sr/^{86}Sr$ composition between normal mid-ocean ridge basalts (~0.7026) and seawater (0.70906) have been widely used to trace seawater-crust interactions [e.g., *Barrett and Friedrichsen*, 1982; *Kawahata et al.*, 1987; *Staudigel et al.*, 1981, 1995, 1996; *Alt et al.*, 1996a; *Hoernle*,

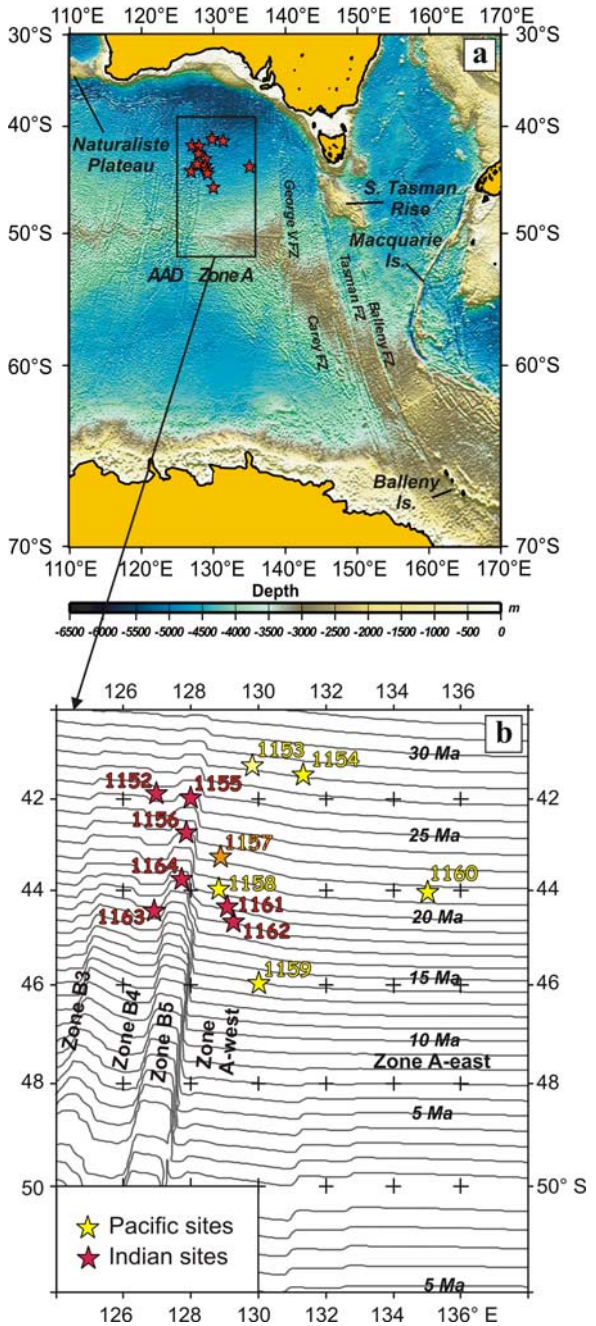

Figure 1. (a) Regional map of the eastern Indian and western Pacific seafloor showing the working area of ODP Leg 187 north of the Southeast Indian Ridge (modified from *Pedersen et al.* [2004]. (b) Map showing locations of ODP Leg 187 drill sites relative to 1 m.y. seafloor isochrones (gray lines). Red and yellow stars represent sites with Indian and Pacific mantle domain characteristics respectively (modified from *Christie et al.* [2001]).

Table 1. Summary of Analyzed Leg 187 Sites

	Site												
	1152AB	1155B	1156A	1157B	1161AB	1163A	1164B	1154A	1157A	1158B	1159A	1160B
Mantle domain	Indian	Indian	Indian	Indian	Indian	Indian	Indian	Pacific	Pacific	Pacific	Pacific	Pacific
Age, Ma	25	24.5	22	22.5	19	17	18–19	28	22.5	21	14	21.5
Sediment thickness, m	A, 0; B, 22.6	149.7	118.2	130.6	A, 116; B, 158.5	161	150.4	233.2	200	126.2	145.6	155
Basement penetration, m	A, 11.2; B, 23.7	46	11.4	40.4	A, 29.3; B, 8.5	47.1	65.7	34.4	16.4	15	27.7	45.1
Recovery, %	A, 5.3; B, 15.1	39.5	55.3	29	A, 15; B, 10.1	33.3	16.2	27.4	17.8	10.7	28.7	28.8
Number of analyzed samples	5	5	3	6	4	4	4	4	2	3	4	9

1998]. In contrast, Nd remains immobile during low-temperature alteration, thus seawater ($^{143}Nd/^{144}Nd = 0.51223$) has no known effect on Nd concentrations and $^{143}Nd/^{144}Nd$ ratios in altered oceanic crust (~0.51300) [e.g., *Staudigel et al.*, 1995; *Hoernle*, 1998; *Hauff et al.*, 2003]. Therefore Nd serves as an excellent reference element to chart the source composition of the oceanic crust.

2. Geological Setting

[5] The study area lies within the Australian Antarctic Discordance (AAD) that is located along the Southeast Indian Ridge (SEIR), between 115°E and 130°E longitudes, at the apex of a westward pointing, V-shaped depth anomaly that extends from southern Australia to Antarctica (Figure 1a). It forms an extensive, 600 km long and 25 km wide depression on the seafloor [*Marks et al.*, 1990; *Pyle et al.*, 1992; *Christie et al.*, 1998]. The anomalously deep water depth of the AAD (4–5 km) is thought to result from relatively thin ocean crust lying above unusually cold mantle [*Forsyth et al.*, 1987; *Marks et al.*, 1990]. The bathymetry of the AAD is unusually chaotic and in part similar to that of slow spreading centers with irregular blocks separated by deep axial valleys and mostly bounded by orthogonal spaced scarps [*Christie et al.*, 1998, 2001]. Within the AAD, Pacific MORB source and Indian MORB source mantle domains intertwine [*Klein et al.*, 1988; *Pyle et al.*, 1992] and are readily identified based on chemical differences such as Ba/Zr ratios [*Christie et al.*, 2001] and Nd-Hf-Pb isotope systematics [*Kempton et al.*, 2002].

3. Samples and Analytical Procedures

[6] ODP Leg 187 drilled a total of 23 holes at 13 sites (Figure 1) and recovered 137 m of basaltic core [*Christie et al.*, 2001]. The crustal age of the drill sites is estimated based on their relative position to seafloor magnetic isochrons (Figure 1b) and ranges from ~14 Ma (Site 1159) to ~28 Ma (Sites 1154 and 1153). The sediment thickness ranges from 22 m at Site 1152 to 348 m at Site 1162, but it is not correlated with crustal age (Table 1). Our study is based on 41 whole rock samples from 11 drill sites. Sites 1152, 1155, 1156, 1161, 1163 and 1164 are located in Indian-type ocean crust and Sites 1154, 1158, 1159 and 1160 are in Pacific-type crust. Both mantle domains appear to be present at Site 1157. Because of poor recovery, it was not

Table 2. Description of Analyzed Samples

Sample	Age, Ma	Mantle Domain	Description	Alteration Degree of Analyzed Part
MW8801 27-8	recent	Indian	Pristine AAD glass from recent Southeast Indian Ridge.	glass
MW8801 29-05	recent	Indian	Pristine AAD glass from recent Southeast Indian Ridge.	glass
1152A 1R1 21-25[a]	25	Indian	Aphyric basalt, light gray where weakly altered, orange-brown where very strongly altered. Here small (1 mm) fractures are surrounded by oxidation halos. Pillow fragment.	very strong weak
1152A 1R1 73-77	25	Indian	Aphyric basalt, strongly altered zones are orange brown, medium altered zones are light gray, outer fresh glassy rind covered with palagonite. Pillow fragment.	strong-medium, zoned
1152B 3R1 1-9	25	Indian	Pristine glass from 1-cm-wide glass rim on light gray aphyric basalt. Pillow sequence.	glass
1152B 4R1 79-81	25	Indian	Unaltered, Moderately plagioclase clinopyroxene phyric basalt, light gray. Pillow sequence.	fresh
1155B 2R1 56-60	24.5	Indian	Moderately plagioclase-olivine phyric basalt, very strongly altered to tan brown, altered phenocrysts. Pillow lava.	very strong
1155B 5R2 14-16	24.5	Indian	Moderately plagioclase-olivine phyric basalt, slightly altered to light gray. Pillow lava.	weak
1155B 6R2 14-17	24.5	Indian	Moderately plagioclase-olivine phyric basalt, very strongly altered to light brown, groundmass is affected by oxidation of phenocrysts. Pillow lava.	very strong
1155B 9R2 19-22	24.5	Indian	Pristine glass from a glassy zone (~4 mm thick) of a moderately plagioclase-olivine phyric basalt, slightly altered. Pillow lava.	glass
1155B 9R2 25-29	24.5	Indian	Moderately plagioclase-olivine phyric basalt, slightly altered to grayish, groundmass and olivines are partly altered to Fe-oxyhydroxides. Pillow lava.	medium-weak
1156A 2R2 76-80	22	Indian	Moderately plagioclase-olivine phyric basalt, slightly altered to medium gray. Basalt-carbonate breccia.	weak
1156A 3R1 15-19	22	Indian	Moderately plagioclase-olivine phyric basalt, very strongly altered, brown groundmass. Pillow lava.	very strong
1156A 3R1 140-144	22	Indian	Moderately plagioclase-olivine phyric basalt, slightly altered to medium gray. Pillow lava.	weak
1157B 2R1 10-12	22.5	Indian	Moderately plagioclase-olivine phyric basalt, medium altered to tan brown, olivine in groundmass is replaced by Fe oxyhydroxides. Pillow lava.	medium
1157B 2R1 50-53	22.5	Indian	Moderately plagioclase-olivine phyric unaltered basalt, medium gray. Pillow lava.	fresh
1157B 4R1 136-140[a]	22.5	Indian	Moderately plagioclase-olivine phyric basalt, medium gray where moderately altered, tan brown where strongly altered, glassy rind of ~8 mm thickness. Undefined structure.	glass very strong medium
1157B 8R2 90-93	22.5	Indian	Sparsely to moderately plagioclase-olivine phyric basalt, slightly altered to medium gray. Undefined structure.	weak
1161A 3R1 1-5	19	Indian	Sparsely to moderately plagioclase-olivine phyric basalt, highly altered to brown, pervasive alteration replaces groundmass olivine and clinopyroxene by Fe-oxyhydroxide and brown clay. Talus pile?	very strong

Table 2. (continued)

Sample	Age, Ma	Mantle Domain	Description	Alteration Degree of Analyzed Part
1161A 4R1 86-90	19	Indian	Aphyric basalt, moderately altered to brown color, pervasive replacement of groundmass phases (including clinopyroxene) by Fe-oxyhydroxide+clay, 80% of the olivines are replaced. Basaltic rubble.	strong
1161B 2R1 32-34	19	Indian	Aphyric basalt, moderately altered to medium gray in the center, that is surrounded by a narrow (~5 mm) grayish brown alteration halo. Basaltic rubble.	medium
1161B 3R1 22-25	19	Indian	Moderately to highly plagioclase-olivine phyric basalt, pervasive alteration replacemes groundmass phases with Fe-oxyhydroxide+clay. Olivine phenocrysts are totally replaced by Fe-oxyhydroxides. Basaltic rubble.	strong
1163A 3R1 27-29	17	Indian	Pristine glass from chilled pillow margin (7 mm) of sparsely to moderately plagioclase-olivine phyric basalt, slightly altered to light gray color. Pillow lava.	glass
1163A 6R1 104-109	17	Indian	Medium grained calcareous-clayey sediment, white to pinkish tan color. Sample comes from a ~7mm vein within an aphyric basalt, altered to medium gray for the most part but with brown alteration halo along the vein. Pillow lava.	vein
1163A 8R1 51-56	17	Indian	Aphyric unaltered (gray) basalt with thin (~2 mm) oxidation margin. Pillow lava.	fresh
1163A 9R1 94-97	17	Indian	Aphyric basalt slightly altered to medium gray. Pillow lava.	weak
1164B 8R1 81-86[a]	18-19	Indian	3 mm thick glass rind of an aphyric basalt fragment of sample 1164B 8R1 84-88.	glass
1164B 8R1 84-88[a]	18-19	Indian	Aphyric basalt with light brown groundmass where strongly altered; light gray groundmass where moderately altered. Basaltic rubble.	very strong medium
1164B 10R1 17-20	18-19	Indian	Aphyric basalt, very slightly altered to medium gray, with fresh olivine microphenocrysts. Basaltic rubble.	weak
MW8801 17-33	recent	Pacific	Pristine AAD glass from recent Southeast Indian Ridge	glass
1154A 1W2 82-84	28	Pacific	Very dark brown clay from immediately above the basaltic basement	local sediment
1154A 2R1 75-77	28	Pacific	Moderately plagioclase-olivine phyric basalt, unaltered, light gray groundmass. Pillow lava.	fresh
1154A 5R1 91-93	28	Pacific	Moderately plagioclase-olivine phyric basalt, weakly altered to light gray, olivines phenocrysts replaced by Fe-oxyhydroxide. Pillow lava.	weak
1154A 8R2 51-55	28	Pacific	Moderately plagioclase-olivine phyric basalt, moderately altered to medium gray groundmass, Fe-oxyhydroxide replacement of olivines, very thin glassy rind. Pillow lava.	medium
1157A 2R1 25-27[a]	22.5	Pacific	Aphyric basalt with two alteration domains. Fresh, dark gray core with strongly altered orange margin. In the altered part Fe oxyhydroxides replace groundmass olivine. Clast from a carbonate cemented basalt breccia.	fresh very strong
1158B 4R1 34-38	21	Pacific	Pristine glass from glassy rind on aphyric to sparsely olivine-plagioclase phyric basalt, slightly altered groundmass. Pillow lava.	glass
1158B 4R1 46-48[a]	21	Pacific	Aphyric to sparsely olivine-plagioclase phyric basalt. Inner core is relatively fresh with medium gray groundmass. Margin is strongly weathered to brown, Fe-oxyhydroxide replaced groundmass. Pillow lava.	weak very strong

Table 2. (continued)

Sample	Age, Ma	Mantle Domain	Description	Alteration Degree of Analyzed Part
1159A 5R1 14-19	14	Pacific	Aphyric basalt, medium gray where fresh and light gray where moderately altered, groundmass partially replaced by Fe-oxyhydroxide and yellow-green clay), three open fractures (less than 0.5 mm wide). Pillow lava.	medium fresh
1159A 7R1 14-18[a]	14	Pacific	Aphyric basalt, medium gray moderately altered inner part with brown oxidized margin (~6 mm). Pillow lava.	very strong medium
1160B 2R1 21-25	21.5	Pacific	Aphyric basalt, moderately altered to light gray, groundmass olivine replaced by Fe-oxyhydroxide and clay. Pillow lava.	medium
1160B 4R2 114-119	21.5	Pacific	Moderately plagioclase phyric basalt, moderately altered to medium gray. Pervasive (~30%) groundmass replacement by Fe-oxyhydroxide and smectite. Undefined structure.	medium
1160B 4R2 82-85	21.5	Pacific	Aphyric basalt, outer edge of the sample is very strongly altered and displays extreme iron staining. Massive flow.	very strong
1160B 7R1 9-11[a]	21.5	Pacific	Moderately plagioclase-olivine phyric basalt, groundmass is highly altered to buff color, ~90% of olivine replaced by Fe-oxyhydroxide. Pillow lava.	very strong
1160B 7R1 12-14[a]	21.5	Pacific	Pristine glass from the chilled pillow margin (6 mm) of basalt sample 1160B 7R1 9-11.	glass
1160B 7R1 49-52	21.5	Pacific	Moderately plagioclase phyric basalt, unaltered, gray groundmass. Probably massive flow.	fresh
1160B 9R1 0-2[a]	21.5	Pacific	Chilled margin consists of 4–6 mm clear glass from basalt sample 1160B 9R1 2-4.	glass
1160B 9R1 2-4[a]	21.5	Pacific	Moderately plagioclase-olivine phyric basalt, light brown groundmass where highly altered. Probably pillow lava.	very strong
1160B 9R3 21-26	21.5	Pacific	Aphyric basalt, slightly altered to light gray. Undefined structure.	weak

[a] Samples where variably altered parts were selected from single specimen.

Table 3. Macroscopic Classification Scheme Used to Assign the Degree of Alteration for Samples of This Study

	Description
Fresh	fresh basalt (dark gray to gray) without any secondary phases
Weakly altered	basalts with slight color changes of the groundmass (gray, light gray to medium gray), unaltered phenocrysts
Medium altered	moderate color change of groundmass (medium grey, light brown), groundmass and/or phenocryst replaced by 30–40% Fe-oxyhydroxides and smectites
Strongly altered	strong color change of groundmass (brownish to orange), phenocryst and groundmass replaced by 40–60% Fe-oxyhydroxides and smectites
Very strongly altered	complete color change of groundmass (brown to orange brown), phenocrysts completely replaced by secondary phases (Fe-oxyhydroxide and/or clay)
Vein material	calcareous sediment

always possible to sample fresh glass, fresh basalt and variously altered basalts at each site. Where possible, variably altered parts were preferentially selected from single specimens, and selected pairs are noted in Table 2. From four samples (1157B4R1136-140 and 1164B8R181-86, 84-88 and 1160B 7R1 9-11, 12-14 and 1160B9R10-2, 2-4) fresh glass along with medium to very strongly altered groundmass were obtained. The macroscopically assigned degree of alteration is defined by groundmass color and degree of phenocryst alteration, following the scheme outlined in Table 3. Besides basaltic material, local sediment (1154A1W282-84) and calcareous vein material (from sample 1163A6R1104-109) were also analyzed. In addition three glass samples from the recent SEIR spreading ridge (one from the Pacific (MW880117-33) and two from Indian (MW880127-8 and MW880129-05) mantle domains) were analyzed for Sr-Nd isotopes.

[7] Samples were crushed to millimeter-sized chips, ultrasonically cleaned in distilled water and hand-picked under a binocular microscope in order to split the sample into macroscopically homogenous alteration domains, which were then ground to powder in an agate mortar and mill. Glass chips for isotopic analysis were first leached in cold 6NHCl for 30 minutes to remove possible contamination from handling. Samples were dissolved in hot HF-HNO_3 and Sr-Nd separated following the column chemistry described by *Hoernle and Tilton* [1991]. A total of 56 whole rock powders and glass chips were analyzed for $^{87}Sr/^{86}Sr$ and $^{143}Nd/^{144}Nd$ isotopic compositions by TIMS. On a subset of 43 whole rock powders, Rb, Sr, Sm and Nd concentrations were determined by ICP-MS.

[8] Sr-Nd isotope ratios were analyzed on a Finnigan MAT 262-RPQ^{2+} and TRITON thermal ionization mass spectrometers at IFM-GEOMAR. Sr-Nd isotope ratios were measured in static mode except for multidynamic Nd acquisition on the MAT 262. Sr isotope ratios were normalized within run to $^{86}Sr/^{88}Sr = 0.1194$ and NBS 987 measured along with the samples gave $^{87}Sr/^{86}Sr = 0.710221 \pm 0.000021$ (2 sigma, n = 14) on the MAT 262 and $^{87}Sr/^{86}Sr = 0.710252 \pm 0.000006$ (2 sigma, n = 6) on the TRITON. Sr isotopic ratios are reported relative to $^{87}Sr/^{86}Sr = 0.71025$ for NBS 987. Nd isotope ratios were normalized within run to $^{146}Nd/^{144}Nd = 0.7219$ and standards gave $^{143}Nd/^{144}Nd = 0.511712 \pm 0.000012$ (2 sigma, n = 11) for our in-house SPEX Nd monitor and $^{143}Nd/^{144}Nd = 0.511843 \pm 0.000009$ (2 sigma, n = 4) for La Jolla on the MAT 262 and $^{143}Nd/^{144}Nd = 0.511708 \pm 0.000002$ (2 sigma, n = 3) for our in-house SPEX Nd monitor and $^{143}Nd/^{144}Nd = 0.511844 \pm 0.000007$ (2 sigma, n = 15) for La Jolla on the TRITON.

[9] Rb, Sr, Sm, Nd concentrations were determined on an Agilent 7500c inductively coupled plasma-mass spectrometer (ICP-MS) at the Geological Institute of the University of Kiel using the sample preparation method of *Garbe-Schönberg* [1993]. Instrument stability was monitored by reanalyzing BHVO-1 every 11 samples resulting in a precision of <1–2 % RSD for the elements presented here. Relative to working values of *Govindaraju* [1994] the analytical accuracy for BHVO-1 is within 13% for Rb, 2.6% for Sr, 3% for Nd and 5.4% for Sm (n = 4) and within 18.3% for Rb, 3.5% for Sr, 3.7% for Nd and 2.5% for Sm for BIR-1 (n = 2).

4. Petrography and Mineralogy

[10] The basement rocks sampled during Leg 187 comprise mostly aphyric to moderately phyric pillow basalts that either occur as pillow lava or as basaltic rubble. In addition, basaltic breccias were recovered with diverse sedimentary infill: carbonates, clays and lithic debris as cement [*Christie et al.*, 2001]. Plagioclase and olivine are

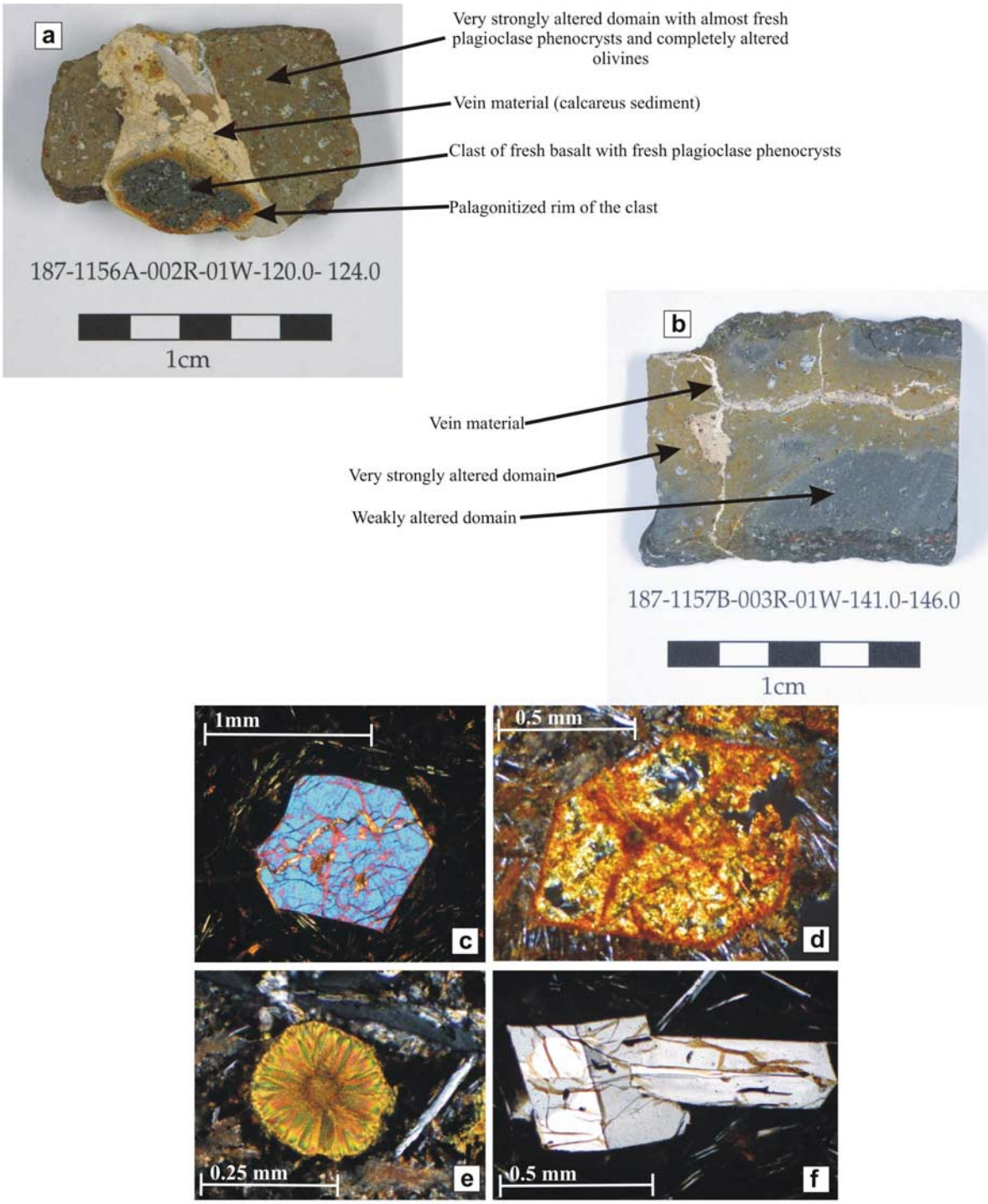

Figure 2. (a and b) Macroscopically visible types of alteration in two representative samples from ODP Leg 187. (c) Cross-polarized light photomicrograph of fresh olivine from unaltered part of the sample 1157A 3R1 25-27. (d) Cross-polarized light photomicrograph of olivine pseudomorphed by smectites and Fe oxides from a very strongly altered part of sample 1157A 3R1 25-27. (e) Cross-polarized light photomicrograph of olivine pseudomorphed by smectites from weakly altered sample 1154A 5R1 91-93. (f) Cross-polarized light photomicrograph of plagioclase with Fe staining along fractures in medium altered sample 1157B 4R1 136-140.

Table 4. The $^{87}Sr/^{86}Sr$ and $^{143}Nd/^{144}Nd$ Compositions and Sr, Rb, Sm, and Nd Concentrations of Samples From ODP Leg 187 (Australian Antarctic Discordance)[a]

Sample	Alteration	Age, Ma	Mantle Domain	Depth, mbsf	Rb, ppm	Sr, ppm	W/R	$^{87}Rb/^{86}Sr$	$^{87}Sr/^{86}Sr$[b]	$^{87}Sr/^{86}Sr$ Initial	Sm, ppm	Nd, ppm	$^{147}Sm/^{144}Nd$	$^{143}Nd/^{144}Nd$[b]	$^{143}Nd/^{144}Nd$ Initial
1152A 1R1 21-25	very strong	25	Indian	0.21	6.64	146	2.08	0.131	0.703651[c](2)	0.703605	5.92	18.3	0.195	0.512939[c](2)	0.512908
1152A 1R1 21-25	weak	25	Indian	0.21	3.04	145	2.11	0.061	0.703665[c](2)	0.703643	5.76	17.4	0.199	0.512951[c](2)	0.512919
1152A 1R1 73-77	strong-medium, zoned	25	Indian	0.73	2.70	138	1.74	0.056	0.703585[c](2)	0.703565	5.56	16.8	0.199	0.512957[c](2)	0.512924
1152B 3R1 1-9	glass	25	Indian	29.81					0.703066(7)					0.512955(7)	
1152B 4R1 79-81	fresh	25	Indian	36.59	2.83	152	2.32	0.054	0.703692[c](3)	0.703673	4.30	13.1	0.198	0.512960[c](2)	0.512928
1155B 2R1 56-60	very strong	24.5	Indian	148.46	3.44	146	1.77	0.068	0.703381(7)	0.703358	2.77	7.86	0.212	0.513035(7)	0.513001
1155B 5R2 14-16	weak	24.5	Indian	161.74	3.20	125	0.98	0.074	0.703197(10)	0.703171	2.22	6.34	0.211	0.513037(8)	0.513003
1155B 6R2 14-17	very strong	24.5	Indian	166.69	3.97	138	2.15	0.083	0.703521(6)	0.703492	2.50	7.00	0.215	0.513027(6)	0.512993
1155B 9R2 19-22	glass	24.5	Indian	181.90					0.702828(7)					0.513040(8)	
1155B 9R2 25-29	medium-weak	24.5	Indian	181.15	1.33	135	1.47	0.029	0.703332(7)	0.703322	2.39	6.75	0.213	0.513037(7)	0.513003
1156A 2R2 76-80	weak	22	Indian	120.46	1.43	152	1.32	0.027	0.703332(9)	0.703323	2.95	8.60	0.206	0.512991(9)	0.512961
1156A 3R1 15-19	very strong	22	Indian	124.75	3.17	172	2.31	0.053	0.703529(7)	0.703513	3.29	9.81	0.202	0.512998(8)	0.512969
1156A 3R1 140-144	weak	22	Indian	126.00	2.39	146	0.93	0.047	0.703233(13)	0.703218	2.82	8.26	0.205	0.513001(8)	0.512971
1157B 2R1 10-12	medium	22.5	Indian	130.70	4.46	158	1.47	0.082	0.703277(7)	0.703251	3.99	11.9	0.201	0.513008(8)	0.512978
1157B 2R1 50-53	fresh	22.5	Indian	131.10	10.4	143	1.06	0.211	0.703195(23)	0.703127	3.51	10.2	0.207	0.513042(8)	0.513012
1157B 4R1 136-140	glass	22.5	Indian	144.36					0.702845(9)					0.513044(5)	
1157B 4R1 136-140	very strong	22.5	Indian	144.36	4.54	161	2.14	0.081	0.703444(7)	0.703418	3.96	11.7	0.204	0.513025(5)	0.512995
1157B 4R1 136-140	medium	22.5	Indian	144.36	2.06	145	1.41	0.041	0.703294(7)	0.703281	3.53	10.4	0.205	0.513033(11)	0.513003
1157B 8R2 90-93	weak	22.5	Indian	163.72	2.15	148	1.26	0.042	0.703243(7)	0.703230	3.57	10.5	0.205	0.513045(8)	0.513015
1161A 3R1 1-5	very strong	19	Indian	120.01	3.34	134	2.42	0.072	0.703597[c](3)	0.703578	4.78	13.5	0.213	0.513030[c](3)	0.513004
1161A 4R1 86-90	strong	19	Indian	130.26	2.45	123	1.71	0.058	0.703437[c](3)	0.703421	3.13	8.72	0.216	0.513046[c](3)	0.513019
1161B 2R1 32-34	medium	19	Indian	158.82	3.87	99.0	0.82	0.113	0.703196[c](1)	0.703166	5.04	14.1	0.216	0.513052[c](2)	0.513025
1161B 3R1 22-25	strong	19	Indian	163.12	4.86	121	1.96	0.116	0.703523[c](2)	0.703491	4.11	11.7	0.211	0.513045[c](2)	0.513019
1163A 3R1 27-29	glass	17	Indian	165.67					0.702927(8)					0.512996(9)	
1163A 6R1 104-109	vein	17	Indian	181.84	29.9	159		0.543	0.711147[c](5)	0.711016	0.99	3.96	0.151	0.512380[c](2)	0.512363
1163A 8R1 51-56	fresh	17	Indian	190.41	2.95	174	1.17	0.049	0.703242(6)	0.703230	3.29	10.1	0.197	0.512969(6)	0.512947
1163A 9R1 94-97	weak	17	Indian	195.04	2.34	169	1.10	0.040	0.703232(7)	0.703222	2.93	8.37	0.211	0.512975(6)	0.512952
1164B 8R1 81-86	glass	18.5	Indian	189.31					0.702901(7)					0.512994(6)	
1164B 8R1 84-88	very strong	18.5	Indian	189.34	1.66	173	1.90	0.028	0.703400(6)	0.703392	3.13	9.74	0.193	0.512986(7)	0.512963
1164B 8R1 84-88	medium	18.5	Indian	189.34	2.28	165	1.66	0.040	0.703363(7)	0.703352	2.85	8.06	0.213	0.512987(9)	0.512961
1164B 10R1 17-20	weak	18.5	Indian	206.97	3.71	144	1.24	0.075	0.703301(7)	0.703281	2.54	7.24	0.212	0.512982(9)	0.512956
MW8801 27-8	glass	recent	Indian						0.702960(8)					0.513035(7)	
MW8801 29-05	glass	recent	Indian						0.702929(6)					0.513041(6)	
1154A 1W2 82-84	sediment	28	Pacific	2.32	153	127		3.506	0.732716(9)	0.731322	11.7	55.8	0.126	0.512110(10)	0.512087
1154A 2R1 75-77	fresh	28	Pacific	233.95	4.51	120	0.99	0.108	0.703051(7)	0.703008	4.62	13.1	0.213	0.513061(5)	0.513022
1154A 5R1 91-93	weak	28	Pacific	247.61	15.1	116	1.30	0.376	0.703183(8)	0.703034	4.31	12.0	0.217	0.513070(8)	0.513030
1154A 8R2 51-55	medium	28	Pacific	263.21	4.53	127	1.77	0.103	0.703298(9)	0.703257	5.05	14.4	0.210	0.513057(6)	0.513018
1157A 2R1 25-27	fresh	22.5	Pacific	200.25	1.36	119	0.75	0.033	0.703145(8)	0.703134	4.35	12.6	0.208	0.513045(8)	0.513014
1157A 2R1 25-27	very strong	22.5	Pacific	200.25	8.10	279	4.78	0.084	0.703599(8)	0.703572	9.68	28.0	0.208	0.513032(8)	0.513001
1158B 4R1 34-38	glass	21	Pacific	137.14					0.702694(6)					0.513046(8)	

Table 4. (continued)

Sample	Alteration	Age, Ma	Mantle Domain	Depth, mbsf	Rb, ppm	Sr, ppm	W/R	$^{87}Rb/^{86}Sr$	$^{87}Sr/^{86}Sr$[b]	$^{87}Sr/^{86}Sr$ Initial	Sm, ppm	Nd, ppm	$^{147}Sm/^{144}Nd$	$^{143}Nd/^{144}Nd$[b]	$^{143}Nd/^{144}Nd$ Initial
1158B 4R1 46-48	weak	21	Pacific	137.26	1.14	124	0.90	0.027	0.703043(7)	0.703035	4.28	12.3	0.210	0.513049(8)	0.513020
1158B 4R1 46-48	very strong	21	Pacific	137.26	2.29	146	3.17	0.045	0.703642(7)	0.703629	5.13	14.7	0.210	0.513042(6)	0.513013
1159A 5R1 14-19	medium	14	Pacific	157.44	3.78	114		0.096	0.703310[c](3)	0.703291	4.77	13.6	0.211	0.513049[c](2)	0.513030
1159A 5R1 14-19	fresh	14	Pacific	157.44	1.47	109		0.039	0.702873[c](3)	0.702865	5.00	14.3	0.210	0.513043[c](4)	0.513024
1159A 7R1 14-18	very strong	14	Pacific	166.84	2.27	121		0.054	0.703546[c](3)	0.703535	6.11	17.6	0.209	0.513013[c](4)	0.512994
1159A 7R1 14-18	medium	14	Pacific	166.84	3.23	112		0.083	0.703359[c](2)	0.703342	4.31	12.2	0.212	0.513049[c](3)	0.513030
1160B 2R1 21-25	medium	21.5	Pacific	160.31	4.04	127	1.19	0.092	0.702965[c](3)	0.702937	2.58	6.81	0.228	0.513057[c](5)	0.513025
1160B 4R2 114-119	medium	21.5	Pacific	172.14	3.45	113	1.12	0.089	0.703019(7)	0.702992	2.07	5.29	0.236	0.513059(5)	0.513026
1160B 4R2 82-85	very strong	21.5	Pacific	171.82					0.703239[c](3)					0.513063[c](3)	
1160B 7R1 9-11	very strong	21.5	Pacific	188.09	2.91	119	3.27	0.071	0.703719(7)	0.703697	2.53	6.30	0.242	0.513056(9)	0.513022
1160B 7R1 12-14	glass	21.5	Pacific	188.12					0.702536(8)					0.513051(7)	
1160B 7R1 49-52	fresh	21.5	Pacific	188.49	0.40	87.1	0.32	0.013	0.702722(7)	0.702718	2.15	5.43	0.238	0.513053(7)	0.513020
1160B 9R1 0-2	glass	21.5	Pacific	177.20					0.702541(8)					0.513055(7)	
1160B 9R1 2-4	very strong	21.5	Pacific	197.22	3.07	121	3.09	0.074	0.703653(7)	0.703630	2.52	6.29	0.241	0.513045(11)	0.513011
1160B 9R3 21-26	weak	21.5	Pacific	200.33					0.702872[c](2)					0.513046[c](2)	
MW8801 17-33	glass	recent	Pacific						0.702506(7)					0.513075(6)	

[a] Incomplete data reflect insufficient sample material. Crustal age is inferred from the seafloor paleomagnetic isochrone map (Figure 1). W/R refers to seawater/rock ratio required to shift $^{87}Sr/^{86}Sr$ from mantle values (inferred from glass data) to $^{87}Sr/^{86}Sr$ of the altered basalt (see text for details).
[b] Values in parentheses are 2 sigma within-run error.
[c] Values were obtained using TRITON; all others are MAT 262 data.

the most common phenocryst phases. Clinopyroxenes were found only in Holes 1152B and 1164A (Figure 1b). Thirty percent of the phenocrysts occur as glomerocrysts, which occur as loose centimeter-sized clusters of prismatic plagioclase and equant olivine or strongly intergrown aggregates. Pillow basalts have microcrystalline groundmass textures, containing plagioclase, olivine and clinopyroxene crystals.

[11] The basalts are altered on a macroscopic scale, recognized as oxidation halos around the margins of samples and along veins and open fractures (Figure 2). On the basis of the type and extent of discoloration, the basalts appear to be variably altered, ranging from virtually pristine (dark gray), through slightly altered (light gray) to completely altered basalts (brown-orange colors). For detailed lithological and petrographic descriptions, see *Christie et al.* [2001]. Common alteration products are Fe-oxyhydroxides and clay minerals (smectite group), both replacing olivine and clinopyroxene phenocrysts and groundmass, and palagonite replacing glass. Occasionally groundmass is replaced with carbonate which is also a common vein filling. These observations indicate alteration in a low-temperature environment. Celadonite, a very common secondary mineral that is often described in other low-temperature alteration studies [e.g., *Marescotti et al.*, 2000], was not identified in Leg 187 samples by standard petrographic methods applied here. Similarly, characteristic dark black halos described elsewhere [e.g., *Talbi and Honnorez*, 2003] were also not present in our sample collection. Brief petrographic descriptions of Leg 187 samples used in this study are listed in Table 2. No systematic changes in the macroscopically visible degree of alteration were observed within or between drill sites. Olivine is most susceptible to alteration in all samples; less sensitive is clinopyroxene and plagioclase phenocrysts appear most resistant [*Miller and Kelley*, 2004]. Plagioclase alteration only occurs as Fe staining along cracks inside crystals (Figure 2f), even in very strongly altered samples with extreme groundmass discoloration to orange-brown. The degree of phenocryst alteration does not always correlate with the degree of groundmass alteration, as partly fresh phenocrysts are sometimes present in strongly altered groundmass.

5. Analytical Results

[12] Sr and Nd isotopic data and Sr, Rb, Sm, Nd concentrations are given in Table 4, together with the macroscopically assigned degree of alteration, age, depth and the calculated seawater/rock ratio of the sample. No correlation exists between any of the studied parameters and borehole depth, most likely reflecting the shallow basement penetration of less than 56m in all sites.

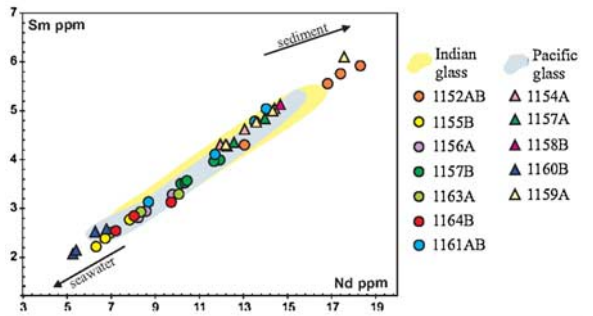

Figure 3. Sm versus Nd concentrations of 43 variably altered basalt samples from 11 drill sites of ODP Leg 187. The yellow field (Indian mantle domain) and light blue field (Pacific mantle domain) are defined by glass data from the same sites (D. Pyle, personal communication, 2002). In Figures 3–7, circles are used for the Indian mantle domain, and triangles are used for the Pacific mantle domain. Arrows point to the positions of seawater and local sediment that lie outside the plot area.

5.1. Sm-Nd and Rb-Sr Concentrations

[13] In general MORB from the Pacific and Indian mantle domains displays a similar range in Sm and Nd element concentrations (Figure 3) in both glass (2.5–5.4ppm Sm, 6.4–16.5ppm Nd) and whole rock (2.1–6.1ppm Sm, 5.3–18.3 Nd) samples. These concentrations are similar to dredge sample data from this region [*Pyle et al.*, 1995; *Klein et al.*, 1988]. The good covariation of Sm and Nd concentration provides additional evidence that these elements are not affected by alteration. Basalts from the Pacific mantle domain generally extend to lower Sr concentrations (87–146 ppm) than those from the Indian mantle domain (125–174 ppm) (Figure 4), possibly reflecting a primary difference between these mantle domains. Rb concentrations in fresh glass range from 0.05 to 0.92 ppm (Pacific domain) and from 0.47 to 1.47 ppm (Indian domain), whereas Rb in the altered basalts is significantly higher, ranging from 2 ppm to 15 ppm. A correlation between Sm, Nd, Sr and Rb contents and crustal age is not observed (Figure 5).

5.2. Nd and Sr Isotopes

[14] The fresh glasses (Figure 6) from the Pacific domain sites have $^{143}Nd/^{144}Nd$ = 0.513009 to 0.513075. Altered and fresh basalts fall within this

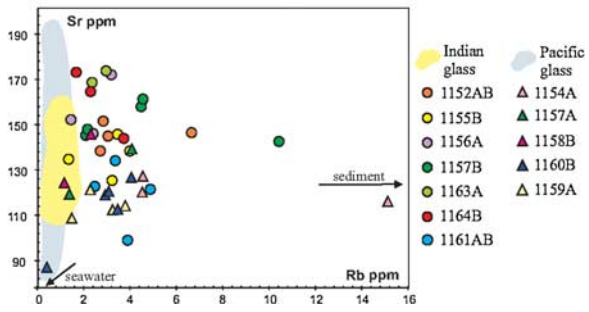

Figure 4. Rb versus Sr concentrations of 43 variably altered basalt samples from ODP Leg 187. The yellow field (Indian mantle domain) and light blue field (Pacific mantle domain) are defined by glass data from the same sites (D. Pyle, personal communication, 2002). Arrows point to the positions of seawater and local sediment that lie outside the actual plot area.

range. The fresh Indian-mantle-type glasses display lower overall $^{143}Nd/^{144}Nd = 0.512921 - 0.513041$ than the Pacific samples and groundmass of Indian-type basalts largely overlaps the glass data ($^{143}Nd/^{144}Nd = 0.512939 - 0.513052$). Glasses and variously altered basalts from both mantle domains have isotopic ratios that lie within the respective fields of on-axis AAD lavas [*Klein et al.*, 1988]. Within single sites, $^{143}Nd/^{144}Nd$ isotopic ratios remain constant within analytical error and thus show no evidence of basalt seawater exchange (Figure 6). Altered samples show the same range of Nd contents and $^{143}Nd/^{144}Nd$, consistent with the idea that seawater alteration has little effect on Nd. No correlation exists between Nd concentrations, $^{143}Nd/^{144}Nd$ or crustal age (Figure 5).

[15] The $^{87}Sr/^{86}Sr$ ratios (Figure 6) for fresh glasses range from 0.70251 to 0.70270 for the Pacific and $^{87}Sr/^{86}Sr = 0.70278$ to 0.70308 for the Indian-mantle-type basalts. Basalts, even when only slightly altered, have higher $^{87}Sr/^{86}Sr$ than the associated glasses. In general the $^{87}Sr/^{86}Sr$ appears to become more radiogenic with the macroscopically increasing degree of alteration (Figure 6e) and thus $^{87}Sr/^{86}Sr$ may serve as chemical proxy for the degree of seawater alteration at a given $^{143}Nd/^{144}Nd$. Exceptions are noted for some macroscopically fresh basalts having similar or even higher Sr isotopic ratios than very strongly altered samples (e.g., Site 1152) which could reflect that some alteration minerals (e.g., smectites) are not

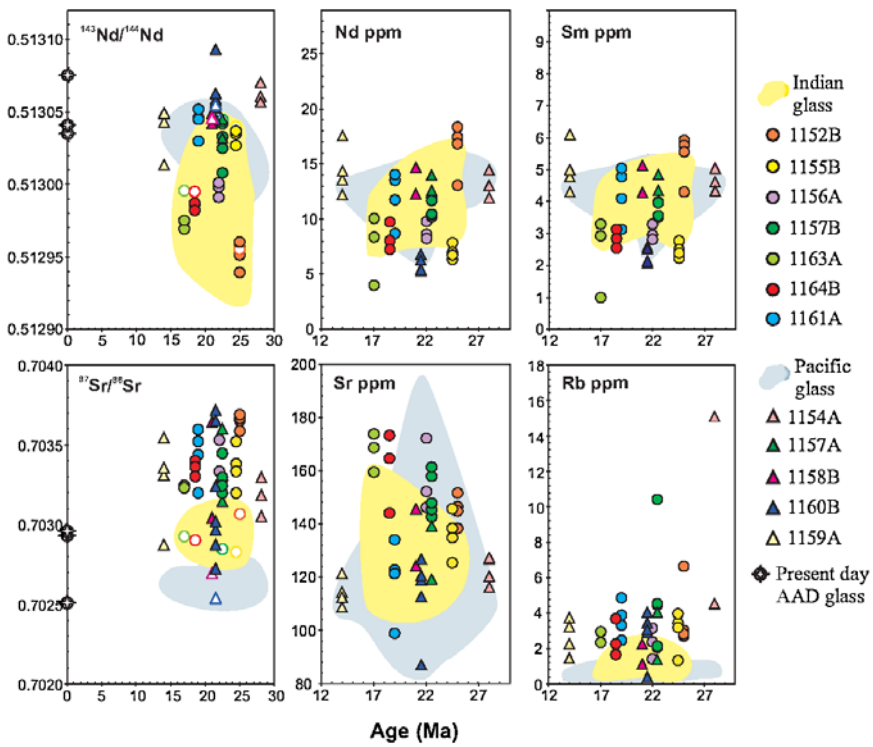

Figure 5. Sr, Rb, Nd, and Sm concentrations, $^{143}Nd/^{144}Nd$ and $^{87}Sr/^{86}Sr$ of ODP Leg 187 basalts against crustal age. The yellow field (Indian mantle domain) and light blue field (Pacific mantle domain) are defined by glass data from the same sites (D. Pyle, personal communication, 2002). Arrows point to the positions of seawater and local sediment that lie outside the actual plot area.

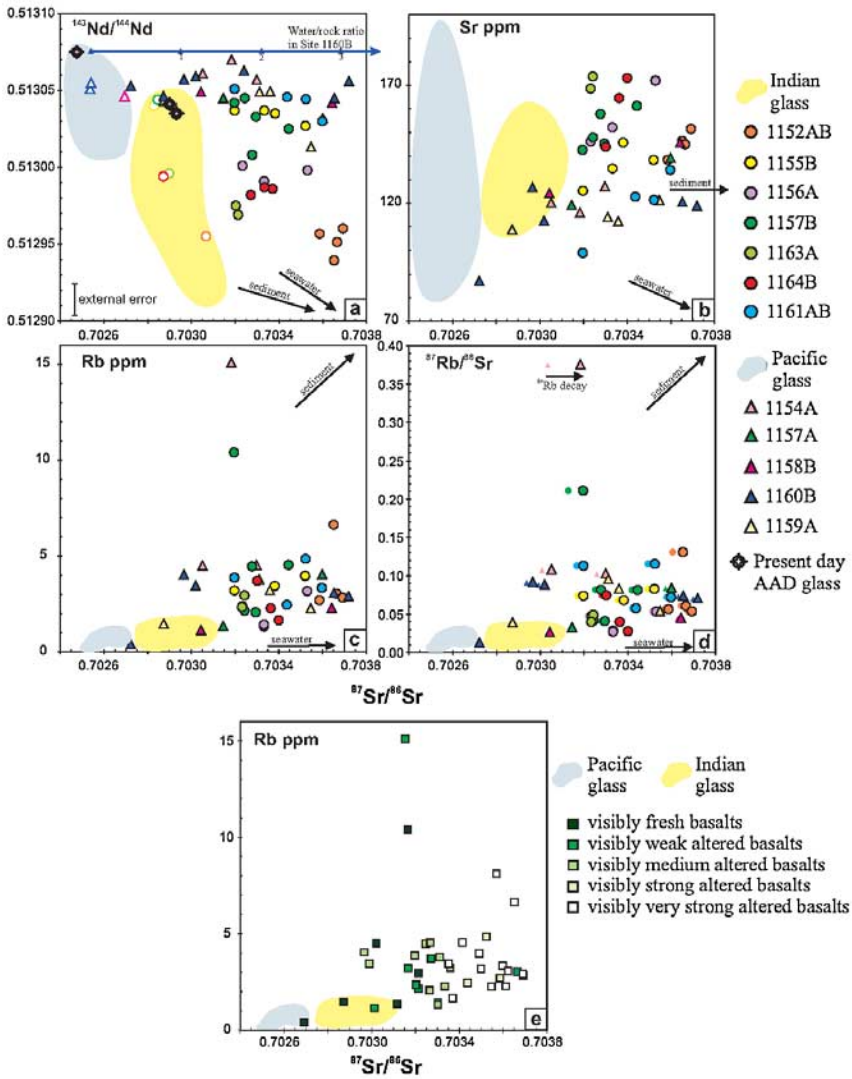

Figure 6. (a) The $^{143}Nd/^{144}Nd$ versus $^{87}Sr/^{86}Sr$ isotopic composition of variably altered basalt samples (solid symbols) and fresh glass (open symbols) from ODP Leg 187. Fields are based on glass data from the same sites (D. Pyle, personal communication, 2002). Also shown are modern AAD glasses for reference. Lavas with Indian mantle characteristics seem to extend to less radiogenic $^{143}Nd/^{144}Nd$ and more radiogenic $^{87}Sr/^{86}Sr$ compositions than those with Pacific mantle characteristics. Within single sites, $^{87}Sr/^{86}Sr$ is generally more radiogenic in whole rock than fresh glass, whereas $^{143}Nd/^{144}Nd$ is homogenous within analytical error, except at site 1157B. The general offset toward more radiogenic $^{87}Sr/^{86}Sr$ in the altered basalts mainly results from addition/exchange of seawater-derived Sr at hydrated interlayer sites during smectite formation. The arrow points toward increasing seawater/rock ratios required to shift $^{87}Sr/^{86}Sr$ from the mantle value of site 1160B (as inferred from site 1160B glass data) to the measured $^{87}Sr/^{86}Sr$ of the altered basalts. (b) Sr concentration versus $^{87}Sr/^{86}Sr$. (c) Rb concentrations versus $^{87}Sr/^{86}Sr$. (d) Plot of $^{87}Rb/^{86}Sr$ versus $^{87}Sr/^{86}Sr$ for measured (black rim) and initial data (no rim). (e) Rb concentration versus $^{87}Sr/^{86}Sr$ with data being sorted by visible degree of alteration. For most samples, no correlation exists between Rb enrichment and degree of alteration. Two samples which appear fresh to weakly altered display the most extreme Rb enrichment and have intermediate $^{87}Sr/^{86}Sr$ compositions. A general overlap in $^{87}Sr/^{86}Sr$ is observed for the fresh through medium altered basalts and the strongly through very strongly altered basalts. Arrows point to the positions of seawater and local sediment that lie outside the actual plot area.

always macroscopically visible. No obvious correlation exists between Sr concentration and $^{87}Sr/^{86}Sr$ ratio or between the $^{87}Sr/^{86}Sr$ ratio and the degree of alteration or the age of the crust (Figure 5). Initial $^{87}Sr/^{86}Sr$ ratios, determined using the measured $^{87}Rb/^{86}Sr$ ratios, are not significantly shifted from the measured $^{87}Sr/^{86}Sr$ values (Figure 6d), indicating that the radiogenic $^{87}Sr/^{86}Sr$

signature in most samples mainly results from exchange with seawater derived Sr rather than from ^{87}Rb decay. Exceptions are, however, noted for samples with $^{87}Rb/^{86}Sr \geq 0.1$ (Figure 6d).

6. Discussion

6.1. Behavior of the Rb-Sr Isotope System During Low-Temperature Alteration

[16] Present-day seawater has a Sr content of 8 ppm and $^{87}Sr/^{86}Sr$ ratio of 0.70906 [*Faure*, 1986], and therefore can have a strong influence on the Sr isotopic composition of the oceanic crust. Sr contents of basalts, however, do not appear to increase even in very strongly altered samples (Figure 6b), indicating that Sr exchange rather than Sr addition [*Kawahata et al.*, 1987] is the main mechanism for elevating $^{87}Sr/^{86}Sr$ in the ocean crust. The most likely explanation for this phenomenon reflects the nature of Sr absorption into smectites and celadonite, although celadonite was not identified in the studied samples. Both smectite and celadonite are very absorbent minerals and incorporate Sr most likely into octahedral sites or as hydrated ions into the interlayer sites [*Staudigel et al.*, 1981]. Sr ions have high hydration energy and produce hydrated interlayers and thus remain exchangeable as long as the basalt-seawater reaction takes place. This mechanism will increase the $^{87}Sr/^{86}Sr$ ratio in the altered basalt due to the exchange with more radiogenic seawater without increasing the total Sr concentration of the rock.

[17] In contrast, the absorption of Rb into smectites and celadonite is restricted to interlayer sites. Rb ions have low hydration energy and are preferentially absorbed into interlayer sites where they cause dehydration and successive layer collapse which structurally fixes Rb [*Staudigel et al.*, 1981]. This mechanism would explain why the concentration of Rb is higher in altered basalt samples. The highest Rb concentrations however are observed in two weakly altered samples: (1157B2R150-53 – 10.4 ppm and 1154A5R191-93 – 15.1 ppm) where the $^{87}Sr/^{86}Sr$ isotopic ratios are relatively low (Figure 6c). Therefore in some cases the addition of Rb into the basalt takes place more rapidly than the $^{87}Sr/^{86}Sr$ exchange with seawater. Moreover the amount of Rb which can be added to smectites is probably unpredictable and not related to the extent of alteration. Otherwise it would be expected that the altered basalts with abundant smectite should have the highest Rb contents. Thus even weakly altered basalts with small amounts of secondary smectites are able to take up large amounts of Rb. Macroscopically fresh samples with high Rb concentrations but "MORB like" $^{87}Sr/^{86}Sr$ are also described from Site 843 and by *King et al.* [1993] and *Waggoner* [1993] (Figure 7b).

[18] Another mechanism affecting the Rb-Sr system in the ocean crust is the precipitation of carbonates during crustal fracturing which can last up to 100 Ma [*Alt and Teagle*, 1999]. According to *Staudigel et al.* [1981], carbonate formation can drastically increase $^{87}Sr/^{86}Sr$ and slightly decrease Rb concentrations but leaves Sr concentrations in the bulk rock relatively unchanged. Calcite-filled fractures play a minor role in ODP Leg 187 basalts and when present were avoided during sample preparation, since this study primarily investigates the effects of groundmass alteration.

6.2. Possible Contaminants

[19] The isotopic composition of the basalts might be influenced by the following contaminants: local sediment, vein material and seawater. Since $^{87}Sr/^{86}Sr$ of the local sediment (0.73272) is much more radiogenic than even in the most altered basalt (0.70372), sediment could serve as a possible mixing end-member. In case of bulk assimilation of sediment, it is expected that $^{143}Nd/^{144}Nd$ of the altered basalt would also shift from mantle values toward those of the local sediment ($^{143}Nd/^{144}Nd = 0.512110$). However, $^{143}Nd/^{144}Nd$ ratios of all fresh and altered basalts remain constant within sites suggesting that bulk sediment assimilation does not play a role. In addition, considering the high Rb (153 ppm), Sm (11.7 ppm) and Nd (55.8 ppm) concentrations in the sediment, bulk assimilation should also have led to a profound increase in the concentration of these elements in the altered basalts, with the greatest increase in Rb and the lowest increase in Sm. The samples however have on average 3.5 ppm Rb, 3.8 ppm Sm and 11 ppm Nd.

[20] The analyzed vein material (clayey calcarenite) at site 1163A comes from a crack within a pillow basalt. Its $^{87}Sr/^{86}Sr$ of 0.71115 is more radiogenic than seawater but much less radiogenic than the local sediment. Since the vein material consists of calcarenite and clay, the observed $^{87}Sr/^{86}Sr$ most likely represents a mixture of seawater derived calcarenite that precipitated from fluids and detrital clays that accumulated in the crack. The $^{143}Nd/^{144}Nd$ composition of the vein

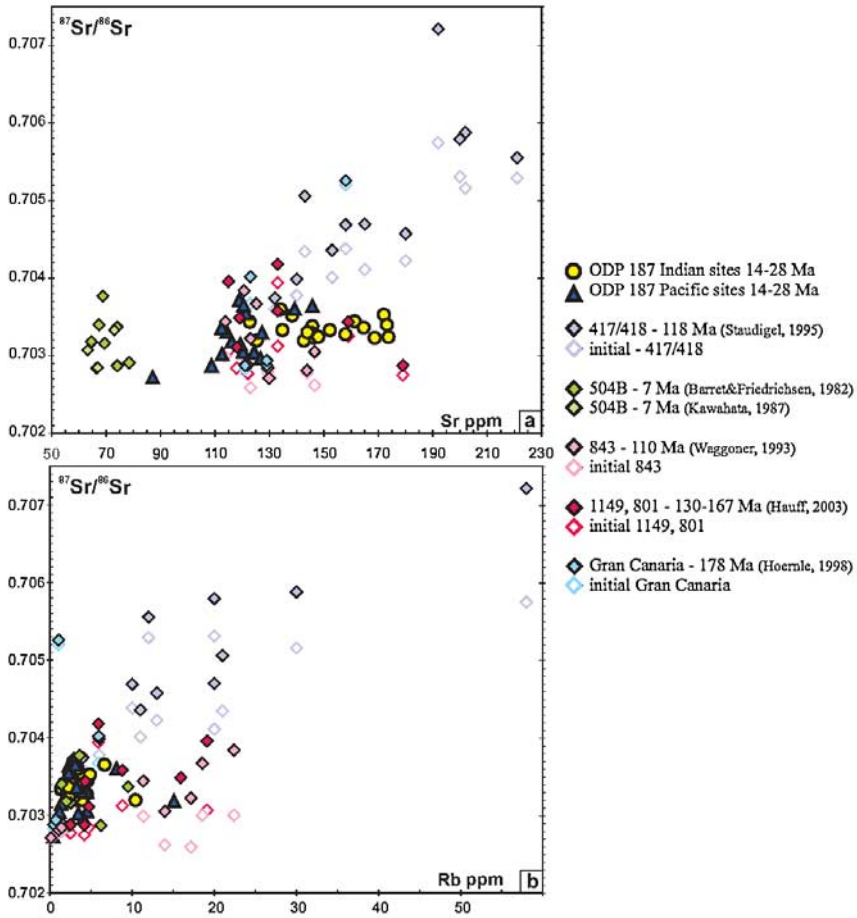

Figure 7. (a) Comparison of Sr contents and $^{87}Sr/^{86}Sr$ of samples from ODP Leg 187 with literature data of young 7 Ma oceanic crust from Hole 504B (Costa Rica Rift) [*Kawahata et al.*, 1987; *Barrett and Friedrichsen*, 1982], 110 Ma crust of the Hawaiian Arch, ODP Site 843 [*Waggoner*, 1993], 118 Ma crust from DSDP/ODP Sites 417/418 (Atlantic crust [*Staudigel et al.*, 1995]), 130–167 Ma basalts from ODP Sites 801 and 1149 (Izu-Bonin-Mariana arc [*Hauff et al.*, 2003; *Kelley et al.*, 2003]), and 178 Ma Jurassic oceanic crust beneath Gran Canaria [*Hoernle*, 1998]. (b) Comparison of Rb contents and $^{87}Sr/^{86}Sr$ of samples from ODP Leg 187 with literature data (data sources are the same as in Figure 7a). Literature data are normalized to $^{87}Sr/^{86}Sr = 0.71025$ for NBS 987.

(0.512380) is higher than seawater (0.512228 [*Frank et al.*, 2002]) and sediment ($^{143}Nd/^{144}Nd$ = 0.512110), suggesting the involvement of radiogenic Nd from basalt in the formation of the vein material. The vein material has low Sm (1 ppm) and Nd (4 ppm) concentrations which are lower than in the basalts and significantly lower than in the sediment reflecting the precipitation of the calcarenite from fluids with low REE contents. The high Rb concentration (30 ppm), however, most likely comes from clayey particles deposited in the crack.

[21] In summary, seawater has high Sr concentration (8 ppm) and radiogenic $^{87}Sr/^{86}Sr$ (0.70906) which can be exchanged with the unradiogenic $^{87}Sr/^{86}Sr$ of the basalts. The Rb concentration in seawater is low (0.11 ppm) but Rb can be increased in basalts through smectite formation. On the other hand, Sm and Nd are fluid immobile elements and their concentrations in seawater (Nd = 2.6×10^{-6} ppm and Sm = 0.545×10^{-6} ppm) are too low to influence the compositions of basalts. Although the long-lasting reaction between seawater and basalt can considerably influence the Nd isotopic composition of seawater [*Staudigel et al.*, 1995], the water/basalt ratio must exceed 10^5 to change Nd isotopic ratios of basalt significantly [*Faure*, 1986]. Consequently, the most probable contaminant for the basalts is seawater. A mixing calculation between seawater and pristine glass shows that the maximum seawater/rock ratio is up to 3 in order to shift the $^{87}Sr/^{86}Sr$ from the local mantle value toward the

most radiogenic $^{87}Sr/^{86}Sr$ of the altered basalt (Figure 6a).

6.3. Comparison With Literature Data of Altered Crust

[22] Figure 7 shows a comparison of our Sr isotope data with literature data of altered oceanic crust of different ages from other DSDP/ODP sites. Despite the huge age difference (7 to 167 Ma) most studies show, similar to our study, increased $^{87}Sr/^{86}Sr$ ratios, increased Rb concentrations and unchanged Sr contents with no intercorrelation of these parameters. An exception is observed for artificial composites from Site 417/418 with much more radiogenic $^{87}Sr/^{86}Sr$, and much higher Rb concentrations. The most reasonable explanation is that interpillow hyaloclastites, which have very radiogenic $^{87}Sr/^{86}Sr$ ratios (e.g., 0.709893) and high Rb abundances [*Hauff et al.*, 2003], were integrated into the composites, pointing out one of the problems in using composite samples.

[23] Basalt-seawater interaction is thought to take place as long as the oceanic crust is permeable. The permeability of the oceanic crust correlates with age and decreases exponentially from 1 Ma to 8 Ma [*Fisher and Becker*, 2000]. The extent of low-temperature alteration is controlled by the type of extrusive material and crustal age [*Jarrard*, 2003] but is probably restricted to the first few million years after eruption of the basalt and finishes when the crust is "corked up" by secondary minerals and overlaying sediment [*Talbi and Honnorez*, 2003]. *Jarrard* [2003] in a numerical model based on matrix densities and potassium contents of smectite, celadonite and fresh basalt, identified that macroporosity and intergranular alteration to smectite, celadonite, and calcite wanes with increasing age. Our $^{87}Sr/^{86}Sr$ data show that the degree of low-temperature alteration in Leg 187 basalts is pervasive, unsystematically distributed and independent of age.

[24] Newly generated oceanic crust is subject to seawater alteration in the vicinity of spreading axes. The longevity of ocean crust alteration depends on the initial permeability of the crust, basement tectonics, spreading rate, sedimentation rate and heat flow, which control the access and circulation of seawater in the crust. When the permeability of the uppermost basaltic crust becomes too low, seawater circulation will cease. Thereafter this altered but impermeable section of the ocean crust will evolve as a closed system with radioactive decay being the only process changing the isotopic composition of this crust. This system can, however, be reopened through tectonic and thermal processes in conjunction with subduction or intraplate volcanism.

7. Conclusions

[25] In the uppermost magmatic portion of ocean crust drilled during ODP Leg 187, no clear correlation exists between various alteration parameters and crustal age in either Pacific- or Indian-type crust, suggesting that the extent of alteration in 14–28 Ma ocean crust is not a function of time. The primary composition of basalts doesn't have any influence on the alteration process, since samples from both mantle domains are altered similarly. The Rb-Sr isotope system appears to be most efficiently altered through exchange with seawater derived Sr and addition of Rb within the first few million years after formation of the ocean crust. Within several million years of formation, the permeability in most oceanic crust will approach zero, thus effectively closing the system to further low-temperature alteration.

[26] In order to estimate the amount of seawater necessary to change $^{87}Sr/^{86}Sr$ from pristine magmatic compositions toward seawater compositions, a water/rock ratio was calculated after *Faure* [1986]:

$$\frac{W}{R} = \left(\frac{\varepsilon_r^i - \varepsilon_r^f}{\varepsilon_r^f - \varepsilon_w^i}\right)\left(\frac{X_r}{X_w}\right),$$

where ε is the isotope ratio of element X and W and R are the weights of seawater and rock. X_r and X_w are the concentrations of element X in rock (r) and water (w) respectively, and the superscripts i and f identify the initial (i) and final (f) values of the epsilon parameters.

Acknowledgments

[27] We thank William M. White (editor), Catherine Chauvel (associate editor), Katherine A. Kelley (reviewer) and an anonymous reviewer for their constructive and positive comments that improved the initial version of this paper. We are grateful to D. Garbe-Schönberg for carrying out trace elements analyses. This study was funded by the Deutsche Forschungsgemeinschaft (grants HA 3097/1-1, 2) and supported by a Ph.D. fellowship grant to Sylwia Krolikowska-Ciaglo by Friedrich-Naumann-Stiftung (resources from German Federal Ministry of Education and Research (BMBF)). This research used samples and/or data provided by the Ocean Drilling Program (ODP). ODP is sponsored by the U.S. National

Science Foundation (NSF) and participating countries under management of Joint Oceanographic Institutions (JOI), Inc.

References

Alt, J. C., and D. A. H. Teagle (1999), The uptake of carbon during alteration of ocean crust, *Geochim. Cosmochim. Acta*, *63*(10), 1527–1535.

Alt, J. C., D. A. H. Teagle, W. Bach, A. N. Halliday, and J. Erzinger (1996a), Stable and strontium isotopic profiles through hydrothermally altered upper oceanic crust, Hole 504 B, *Proc. Ocean Drill. Program Sci. Results*, *148*, 57–69.

Alt, J. C., et al. (1996b), Hydrothermal alteration of a section of upper oceanic crust in the eastern equatorial Pacific: A synthesis of results from Site 504 (DSDP Legs 69, 70, and 83, and ODP Legs 111, 137, 140, and 148), *Proc. Ocean Drill. Program Sci. Results*, *148*, 417–434.

Bach, W., J. C. Alt, Y. Niu, S. E. Humphris, J. Erzinger, and H. J. B. Dick (2001), The geochemical consequences of late-stage low-grade alteration of lower ocean crust at the SW Indian Ridge: Results from ODP Hole 735 (Leg 176), *Geochim. Cosmochim. Acta*, *65*, 3267–3287.

Bach, W., B. Peucker-Ehrenbrick, S. R. Hart, and J. S. Blusztajn (2003), Geochemistry of hydrothermally altered oceanic crust: DSDP/ODP Hole 504B—Implications for seawater-crust exchange and Sr- and Pb-isotopic evolution of the mantle, *Geochem. Geophys. Geosyst.*, *4*(3), 8904, doi:10.1029/2002GC000419.

Barrett, T. J., and H. Friedrichsen (1982), Strontium and oxygen isotopic composition of some basalts from Hole 504B, Costa Rica Rift, DSDP Legs 69 and 70, *Earth Planet. Sci. Lett.*, *60*, 27–38.

Christie, D. M., B. P. West, D. G. Pyle, and B. B. Hanan (1998), Chaotic topography, mantle flow and mantle migration in the Australian-Antarctic discordance, *Nature*, *394*, 637–644.

Christie, D. M., et al. (2001), *Proceedings of the Ocean Drilling Program, Initial Reports* [Online], vol. 187, Ocean Drill. Program, College Station, Tex. (Available at http://www-odp.tamu.edu/publications/187_IR/187ir.htm)

Faure, G. (1986), *Principles of Isotope Geology*, John Wiley, Hoboken, N. J.

Fisher, A. T., and K. Becker (2000), Channelized fluid flow in oceanic crust reconciles heat flow and permeability data, *Nature*, *403*, 71–74.

Forsyth, D. W., R. L. Ehrenbard, and S. Chapin (1987), Anomalous upper mantle beneath the Australian-Antarctic discordance, *Earth Planet. Sci. Lett.*, *84*, 471–478.

Frank, M., N. Whiteley, S. Kasten, J. R. Hein, and K. O'Nions (2002), North Atlantic Deep Water export to the Southern Ocean over the past 14 Myr: Evidence from Nd and Pb isotopes in ferromanganese crusts, *Paleoceanography*, *17*(2), 1022, doi:10.1029/2000PA000606.

Garbe-Schönberg, C.-D. (1993), Simultaneous determination of thirty-seven trace elements in twenty-eight international rock standards by ICP-MS, *Geostand. Newsl.*, *17*, 81–97.

Govindaraju, K. (1994), Compilation of working values and sample description for 383 geostandards, *Geostand. Newsl.*, *18*, 1–158.

Hauff, F., K. Hoernle, and A. Schmidt (2003), Sr-Nd-Pb composition of Mesozoic Pacific oceanic crust (Site 1149 and 801, ODP Leg 185): Implications for alteration of ocean crust and the input into the Izu-Bonin-Mariana subduction system, *Geochem. Geophys. Geosyst.*, *4*(8), 8913, doi:10.1029/2002GC000421.

Hoernle, K. (1998), Geochemistry of Jurassic oceanic crust beneath Gran Canaria (Canary Islands): Implications for crustal recycling and assimilation, *J. Petrol.*, *39*(5), 859–880.

Hoernle, K. A., and G. R. Tilton (1991), Sr-Nd-Pb isotope data for Fuerteventura (Canary Islands) basal complex and subaerial volcanics:applications to magma genesis and evolution, *Schweiz. Mineral. Petrogr. Mitt.*, *71*, 3–18.

Jarrard, R. D. (2003), Subduction fluxes of water, carbon dioxide, chlorine, and potassium, *Geochem. Geophys. Geosyst.*, *4*(5), 8905, doi:10.1029/2002GC000392.

Johnson, H. P., and S. W. Semyan (1994), Age variations in the physical properties of oceanic basalts: Implications for crustal formation and evolution, *J. Geophys. Res.*, *99*, 3123–3134.

Kawahata, H., M. Kusakabe, and Y. Kikuchi (1987), Strontium, oxygen, and hydrogen isotope geochemistry of hydrothermally altered and weathered rocks in DSDP Hole 504B, Costa Rica Rift, *Earth Planet. Sci. Lett.*, *85*, 343–355.

Kelley, K. A., T. Plank, J. Ludden, and H. Staudigel (2003), Composition of altered oceanic crust at ODP Sites 801 and 1149, *Geochem. Geophys. Geosyst.*, *4*(6), 8910, doi:10.1029/2002GC000435.

Kempton, P. D., J. A. Pearce, T. L. Barry, J. G. Fitton, C. Langmuir, and D. M. Christie (2002), Sr-Nd-Pb-Hf isotope results from ODP Leg 187: Evidence for mantle dynamics of the Australian-Antarctic Discordance and origin of the Indian MORB source, *Geochem. Geophys. Geosyst.*, *3*(12), 1074, doi:10.1029/2002GC000320.

King, A. J., D. G. Waggoner, and M. O. Garcia (1993), Geochemistry and petrology of basalts from Leg 136, central Pacific Ocean, *Proc. Ocean Drill. Program Sci. Results*, *136*, 107–118.

Klein, E. M., C. H. Langmuir, A. Zindler, H. Staudigel, and B. Hamelin (1988), Isotope evidence of mantle convection boundary at the Australian-Antarctic Discordance, *Nature*, *333*, 623–629.

Marescotti, P., D. A. Vanko, and R. Cabella (2000), From oxidazing to reducing alteration: Mineralogical variations in pillow basalts from the east flank, Juan de Fuca Ridge, *Proc. Ocean Drill. Program Sci. Results*, *168*, 119–136.

Marks, K. M., P. R. Vogt, and S. A. Hall (1990), Residual depth anomalies and the origin of the Australian-Antarctic Discordance Zone, *J. Geophys. Res.*, *95*, 17,325–17,337.

Miller, D. J., and J. Kelley (2004), Low-temperature alteration of basalt over time: A synthesis of results from Ocean Drilling Program Leg 187, *Proc. Ocean Drill. Program Sci. Results* [Online], *187*. (Available at http://www-odp.tamu.edu/publications/187_SR/206/206.htm)

Pedersen, R. B., D. M. Christie, and D. G. Pyle (2004), Regional and local mantle heterogeneities associated with the Australian Antarctic Discordance: Sr and Nd isotopic results from ODP Leg 187, *Proc. Ocean Drill. Program Sci. Results* [Online], *187*. (Available at http://www-odp.tamu.edu/publications/187_SR/VOLUME/205/205.htm).

Pyle, D. G., D. M. Christie, and J. J. Mahoney (1992), Resolving an isotopic boundary within the Australian-Antarctic Discordance, *Earth Planet. Sci. Lett.*, *112*, 161–178.

Pyle, D. G., D. M. Christie, J. J. Mahoney, and R. A. Duncan (1995), Geochemistry and geochronology of ancient southwest Indian and southwest Pacific seafloor, *J. Geophys. Res.*, *100*, 22,261–22,282.

Schmincke, H.-U., A. Klügel, T. H. Hansteen, K. Hoernle, and P. Bogaard (1998), Samples from the Jurassic ocean crust beneath Gran Canaria, La Palma and Lanzarote (Canary Islands), *Earth Planet. Sci. Lett.*, *163*, 343–360.

Staudigel, H., S. R. Hart, and S. H. Richardson (1981), Alteration of the oceanic crust: Processes and timing, *Earth Planet. Sci. Lett.*, *52*, 311–327.

Staudigel, H., G. R. Davies, R. H. Stanley, K. M. Marchant, and B. M. Smith (1995), Large scale isotopic Sr, Nd and O isotopic anatomy of altered oceanic crust: DSDP/ODP sites 417/418, *Earth Planet. Sci. Lett.*, *130*, 169–185.

Staudigel, H., T. Plank, B. White, and H. U. Schmincke (1996), Geochemical fluxes during seafloor alteration of the basaltic upper oceanic crust: DSDP Sites 417 and 418, in *Subduction: Top to Bottom*, *Geophys. Monogr. Ser.*, vol. 96, pp. 19–38, edited by G. E. Bebout et al., AGU, Washington, D. C.

Talbi, E. H., and J. Honnorez (2003), Low-temperature alteration of mesozoic oceanic crust, Ocean Drilling Program Leg 185, *Geochem. Geophys. Geosyst.*, *4*(5), 8906, doi:10.1029/2002GC000405.

Waggoner, D. G. (1993), The age and alteration of central Pacific Oceanic crust near Hawaii, Site 843, *Proc. Ocean Drill. Program Sci. Results*, *136*, 119–132.

Zhou, W., R. Van der Voo, D. R. Peacor, D. Wang, and Y. Zhang (2001), Low-temperature oxidation in MORB of titanomagnetite to titanomaghemite: A gradual process with implications for marine magnetic anomaly amplitudes, *J. Geophys. Res.*, *106*, 6409–6421.